ACOUSTICS 2012

The parametric propagation in underwater acoustics: experimental results

E. Bouttard[a], V. Labat[a], O. Bou Matar[b] and T. Chonavel[c]

[a]Institut de Recherche de l'Ecole Navale (EA 3634), BCRM Brest CC 600 29240 Brest Cedex 9

[b]Institut d'électronique, de microélectronique et de nanotechnologie, avenue Poincaré, Cité scientifique, BP 69, 59652 Villeneuve d'Ascq cedex

[c]Département Signal et Communications, Technopôle Brest-Iroise CS 83818 29238 Brest Cedex 3

etienne.bouttard@ecole-navale.fr

In underwater acoustics, detection of buried objects in sediments (cables, mines, ...) is a complex problem. Indeed, in order to ensure sufficient penetration depth in marine sediments, low frequencies have to be used, implying a low resolution. A solution proposed to solve this problem is the parametric emission based on the nonlinear properties of seawater. This method can generate a low frequency wave from two directional high frequencies beams.
The aim of this work is to present experimental results of a parametric propagation. Experiments have been carried out in a water tank in various configurations. These experimental measurements are then compared with simulation results obtained with a numerical model based on a fractional-step method presented at the Underwater Acoustic Measurements conference in 2011.

1 Introduction

In order to detect buried objects in marine sediments, low frequency has to be used, implying a low resolution. A solution to solve this problem is the parametric emission. The aim of this work is to present experimental results of a parametric propagation.

A model based on a fractional-step numerical method introduced by Christopher and Parker [1] was presented at the Underwater Acoustic Measurements conference in 2011 [2]. In this method, the normal particle velocity is calculated plane by plane from the source to a specified distance. The effects of nonlinearity, attenuation and diffraction are calculated independently for each spatial step.

A measurement campaign has been conducted to obtain the pressure fields of the primary and parametric frequencies.

Experimental results are then compared with simulation ones.

The present paper is organized as follows : first, the principle of the model is quickly described. Then, after an experimental set up presentation, experimental results are showed for parametric emission in water tank.

2 Numerical modeling

Numerical modeling previously proposed [2] for nonlinear propagation is a frequency domain approach based on the Burgers equation and the angular spectrum method. A numerical solution of Burgers equation is obtained with a split-step operator. Over sufficiently small steps, the effects of nonlinearity, diffraction and attenuation can be treated independently. Knowing the normal velocity field for a plane z , the particle velocity profile v at position $z + \delta z$ is given by [3] :

$$v(z+\delta z) = v(z) + \left(\widehat{L_A}\cdot v + \widehat{L_N}\cdot v + \widehat{L_D}\cdot v\right)\delta z \qquad (1)$$

where $\widehat{L_A}$, $\widehat{L_N}$ and $\widehat{L_D}$ are respectively the attenuation operator, the nonlinear operator and the diffraction operator wich expressions are detailed in [2], [4] and [5].

The propagation modeling is divided into three steps [3] : diffraction over substep $\frac{\delta z}{2}$, nonlinearity and attenuation over δz, and second diffraction over substep $\frac{\delta z}{2}$.

Moreover, several substeps are used for the calculation of the nonlinearity and attenuation effects over the distance δz in order to improve the stability of the code .

To model nonlinear propagation, the wave is decomposed into different harmonic components :

$$v(x,y,z,t) = \frac{1}{2}\sum_{n=-\infty}^{+\infty} v_n(x,y,z)\mathrm{e}^{j\omega_n t} \qquad (2)$$

where $v_n(x,y,z) = |v_n|\,\mathrm{e}^{j\phi_n(x,y,z)}$ and $\phi_n(x,y,z)$ are respectively the complex amplitude and the phase of the n$^{\text{th}}$ harmonic ($\omega_n = n\omega$) at the point (x,y,z). The equation (2) allows to take into account possible inclination and focalization of the transducer [2].

In the case of a parametric emission, two high frequency waves f_{h_1} and f_{h_2} are emitted in order to generate a wave at beating frequency $f_l = f_{h_1} - f_{h_2}$ (with $f_{h_2} > f_{h_1}$) by nonlinear interactions.

The parametric ratio p is defined as the ratio between the average of primary frequencies over parametric frequency :

$$p = \frac{f_h}{f_l} \text{ with } f_h = \frac{f_{h_1} + f_{h_2}}{2} \qquad (3)$$

In order to avoid creating even lower frequencies than f_l by interactions between harmonics, parametric ratio is a half-integer : $p = n + \frac{1}{2}$ with n as a non-zero integer [6]. In this case, f_{h_1} and f_{h_2} are multiples of the parametric frequency : $f_{h_1} = (p - \frac{1}{2})f_l$ and $f_{h_2} = (p + \frac{1}{2})f_l$.

On the transducer surface, only the primary frequencies harmonics components are initilazed, the other components are equal to zero.

The numerical model can take into account the transmission at the water/sediment interface and propagation in the sediments [2]. In the following of this paper, only the results in the water are presented.

3 Experimental set up

Experimental measurements are performed in a water tank of 1.5m × 1.5m × 1m filled with fresh water. The water temperature is about 12 °C and measured celerity is $c_0 = 1450\,\mathrm{m.s^{-1}}$.

A global scheme of the device is shown in Figure 1

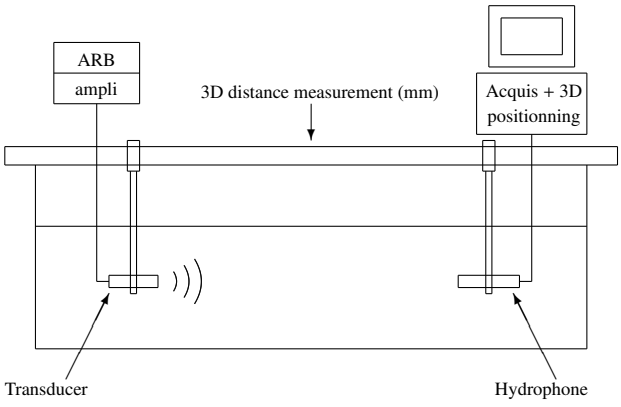

Figure 1: Experimental configuration

A 3D positioning system is used to move the transducer.

An arbitrary waveform generator (*BNC* 625A) is used to provide a synthetic signal wich is the sum of the two primary frequencies (Figure 2).

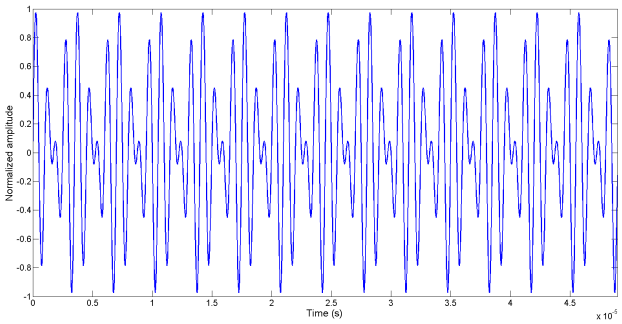

Figure 2: Normalized emitted signal for an average value of the primary frequencies f_h = 1 MHz.

This signal is then amplified by a linear power amplifier (*ENI* AQ-300 RF) with a gain of 55 dB and applied to the transducer.

Two circular piston transducers, with a diameter of 0.5 inch, are used (*Valpey-Ficher* ISO104GP and ISO204HR). Nominal frequencies of the tranducers are respectively 1 MHz and 2.25 MHz.

The sound pressure fields generated in water are measured with two hydrophones (Figure 3) : a needle hydrophone (*Precision Acoustics* PVDF ultrasonic SN 950) for the primary frequencies and a *Reson* TC4034 for the parametric frequency.

Figure 3: The two hydrophones used : *Precision Acoustics* PVDF ultrasonic SN 950 (top) and *Reson* TC4034 (bottom).

The signals measured by the hydrophones are visualized on an oscilloscope (*Tektronix* TDS-3014b) connected to a computer by a GPIB port for acquisition and treatment.

4 Results

The first test was conducted for an average frequency f_h = 1 MHz. The parametric ratio p is 3.5 and the parametric frequency is f_l = 285 kHz.

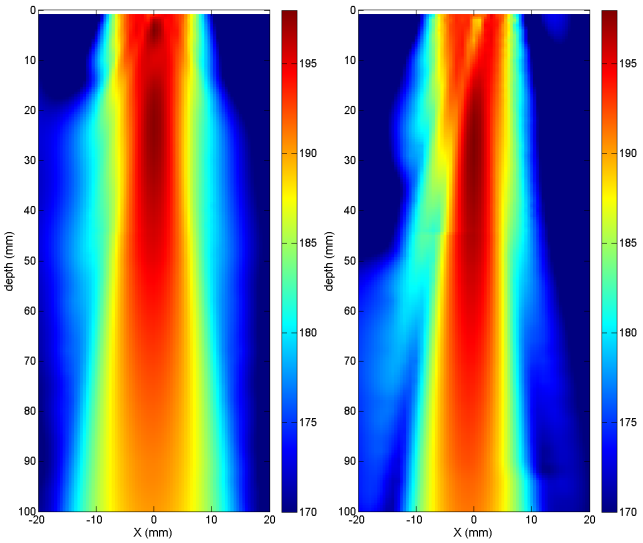

Figure 4: Experimental pressure fields (dB ref 1 µPa) for the primary frequencies at 0.86 MHz (left) and 1.14 MHz (right).

Figure 4 shows the measured pressure fields for the primary frequencies at 0.86 MHz and 1.14 MHz. The highest levels measured, of about 198 dB, occur around the Fresnel distances : between 1.5 and 4 cm for f_1 = 0.86MHz and between 2 and 5 cm for f_2 = 1.14MHz.As expected, the beam is narrower for the higher frequency.

The measured pressures for the primary frequencies are input to theorical model to compare experimental and theorical results.

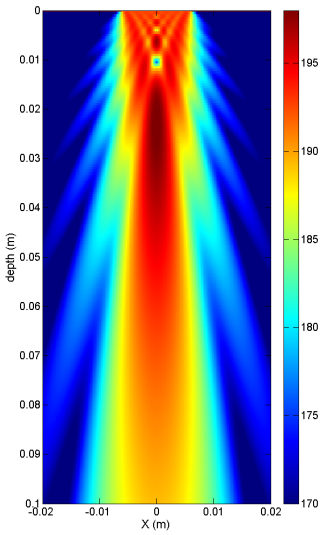

Figure 5: Theorical pressure field (dB ref 1 µPa) for the primary frequency at 0.86 MHz.

Figure 5 shows the theorical field for the first primary frequency. The diffraction figure is more detailed on the theorical pressure field but the level values, the beam size and the position of the maximum value are the same than experimental measurement.

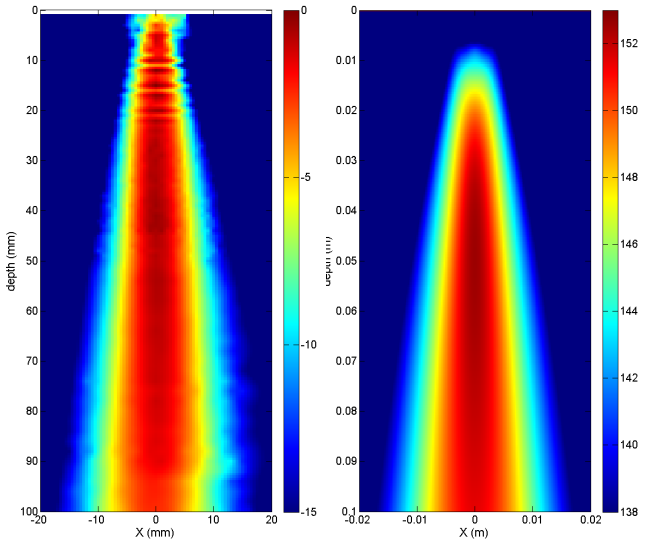

Figure 6: Normalized experimental pressure field (dB) (left) and theorical pressure field (dB ref 1 μPa) (right) for the parametric frequency (285 kHz).

Experimental and theorical pressure fields are presented in figure 6 for the parametric frequency at 285 kHz. The measured pressure field has been normalized because the sensibility of the hydrophone need to be checked.

In the theorical field, there is an increase of the level in the interaction area of the primary frequencies. However, measured level is higher than expected in the near field, which is confirmed in normalized axial evolution curves presented in figure 7.

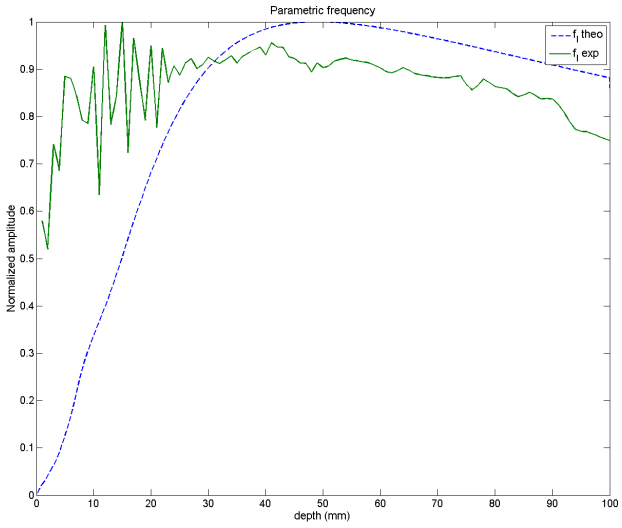

Figure 7: Theorical and experimental axial propagation curves for the parametric frequency.

The axial evolution of the experimental and theorical normalized levels of the primary frequencies are presented in figure 8. There is a distance shift for the maximum value of the second primary frequency probably due to the precision of the celerity measure or a bad alignment between transducer and hydrophone.

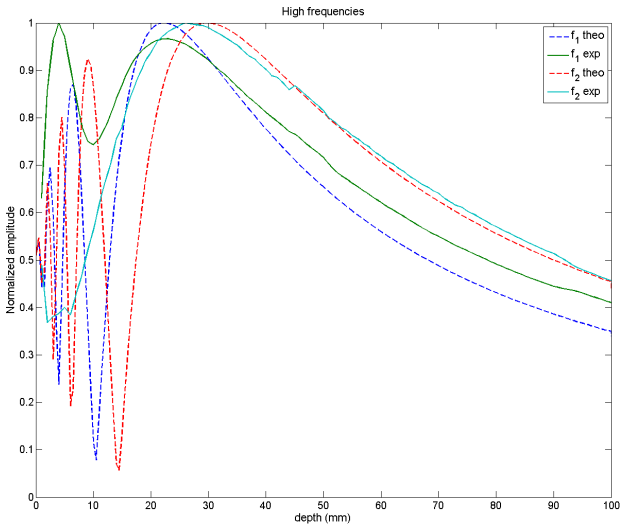

Figure 8: Theorical and experimental axial propagation curves for the primary frequencies.

Beam patterns for the primary and parametric frequencies are respectively presented in figures 9 and 10.

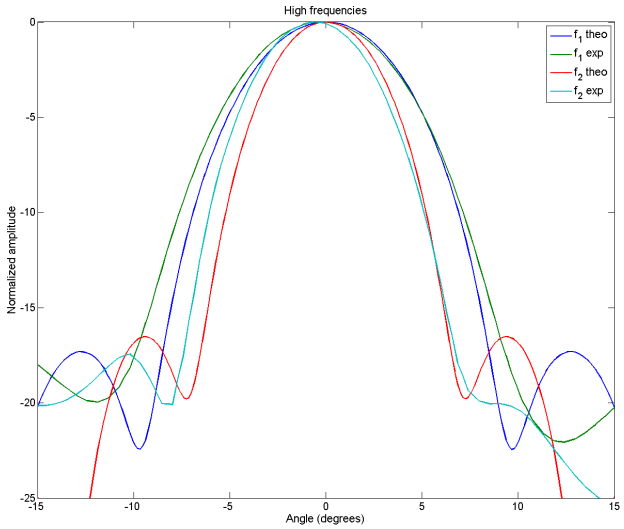

Figure 9: Theorical and experimental normalized beam patterns for the primary frequencies at 0.86 MHz and 1.14 MHz.

Beamwidths for the primary frequencies are respectively 6° for 0.86 MHz and 8° for 1.14 MHz. For the parametric frequency, experimental beamwidth is 7° and there is no sidelobe.

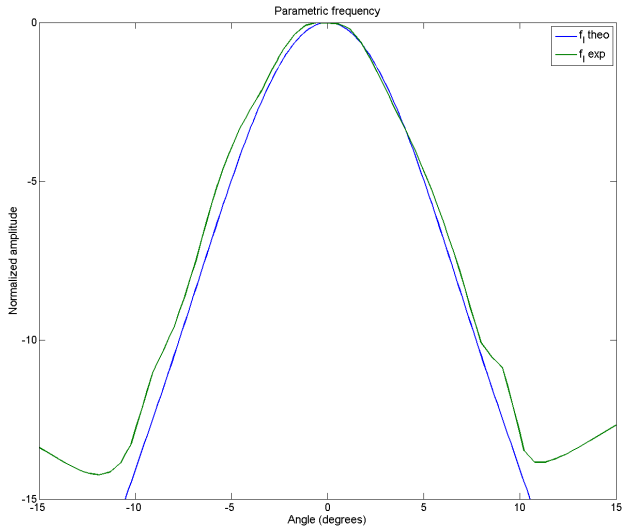

Figure 10: Comparison of experimental and theorical normalized beam patterns for the parametric frequency at 285 kHz.

The second test was conducted for an average frequency f_h = 2.25 MHz. The parametric ratio is 7.5 and the parametric frequency is f_l = 300 kHz.

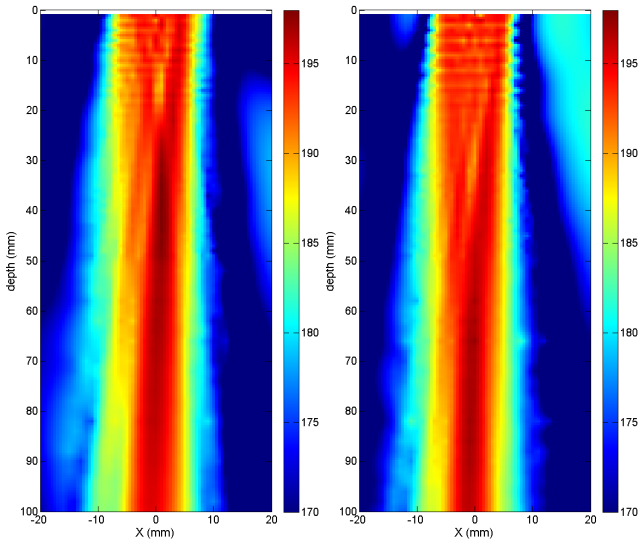

Figure 11: Measured pressure fields (dB ref 1 µPa) for the primary frequencies at 2.1 MHz (left) and 2.4 MHz (right).

Measured pressure fields obtained for an average frequency of 2.25 MHz are presented in figure 11 for the primary frequencies and in figure 12 for the parametric one. A little inclination of the transducer can be observed. As expected, the Fresnel distance is higher, which implies than parametric effects occur further, and the beamwidth is lower (3°) for the primary and parametric frequencies than an average frequency of 1 MHz.

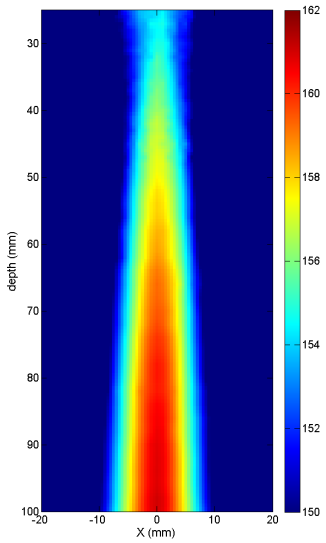

Figure 12: Measured pressure field (dB ref 1 µPa) for the parametric frequency (300 kHz).

5 Conclusion

Experiments have been carried out in a water tank. Experimental results were been compared with simulation ones for a parametric emission.

If general evolutions of the pressure fields are in agreement with the theorical results, unfortunately there is a significant difference for the parametric level. The problem may be due to changes in the hydrophone calibration.

The next set of measure have to be carried out in sediments (sand) for buried object detection.

References

[1] P. T. Christopher, K. J. Parker, "New approaches to nonlinear diffractive field propagation", *J. Acoust. Soc. Am.* **90**, 488-499 (1991)

[2] E. Bouttard, V. Labat, O. Bou-Matar, "Numerical modeling of underwater parametric propagation to detect buried objects", *Proceedings of the 4th Underwater Acoustics Measurements conference*, Kos, Greece (2011)

[3] R. J. Zemp, J. Tavakkoli, R. S. C. Cobbold, "Modeling of nonlinear ultrasound propagation in tissue from array transducers", *J. Acoust. Soc. Am.* **113**, 139-152 (2003)

[4] J. D. Gaskill, *Linear Systems, Fourier Transforms, and Optics*, Wiley (1978)

[5] M. E. Haran, B. D. Cook, "Distorsion of finite amplitude ultrasound in lossy media", *J. Acoust. Soc. Am.* **73**, 774-779 (1983)

[6] J. Marchal, *Acoustique non-linéaire : contribution théorique et expérimentale à l'étude de l'émission paramétrique*, PhD Thesis, Université Paris 6 (2002)